A comprehensive framework of building model reconstruction from airborne LiDAR data

Y Xiao[1,2], C Wang[1], X H Xi[1] and W M Zhang[3]

[1] Center for Earth Observation and Digital Earth, Chinese Academy of Sciences, Beijing, China.

[2] University of Chinese Academy of Sciences, Beijing, China.

[3] Beijing Normal University, Beijing, China

Email: xiaoyong298@gmail.com

Abstract. This paper presents a comprehensive framework of reconstructing 3D building models from airborne LiDAR data, which involves building extraction, roof segmentation and model generation. Firstly, building points are extracted from LiDAR point clouds by removing walls, trees, ground and noises. Walls and trees are identified by the normal and multi-return features respectively and then ground and noise are detected by the region growing algorithm which aims at extracting smooth surfaces. Then the connected component analysis is performed to extract building points. Secondly, once the building points are acquired, building roofs are separated by the region growing algorithm which employs the normal vector and curvature of points to detect planar clusters. Finally, by combining regular building outlines obtained from building points and roof intersections acquired from the roof segmentation results, 3D building models with high accuracy are derived. Experimental results demonstrate that the proposed method is able to correctly obtain building points and reconstruct 3D building models with high accuracy.

1. Introduction

Three dimensional (3D) building models have a wide range of applications such as urban planning, virtual city tourism and emergency decision. However, reconstruction of building model in large urban area is still a challenge task by traditional ways, e.g. photogrammetry. Due to its high precision and fast acquisition time, airborne LiDAR (Light Detection And Ranging) system has become an important data source for 3D building model reconstruction[1]. The generation of 3D building models from airborne LiDAR data mainly involves three key steps, i.e. building detection, roof segmentation and model generation. Various methods which focus on individual aspect have been proposed. For example, [2-5] present building extraction methods by utilizing image classification techniques, e.g. object-based classification. [6-9] describe building roof segmentation methods by several common used segmentation method, e.g. RANSAC, Hough transform and fuzzy c-means. [10-12] present the building boundary extraction and outlines regularization methods which are of high significance in model generation.

This paper proposes a comprehensive framework of reconstructing 3D building models from airborne LiDAR data. In order to extract building points, we utilize reliable features to remove corresponding non-building objects. For example, apparent wall and tree points are detected and removed by the normal and multi-return feature respectively. Then the ground points are identified by the region growing algorithm by detecting huge smooth surfaces. After building points are extracted, building roofs are segmented by a region growing algorithm which aims at extracting planar objects. Meanwhile, regular building boundaries are obtained by adjusting long segments extracted by the RANSAC algorithm. At last, 3D building models are acquired by combining the regularized boundaries and the roof intersections estimated from the roof segmentation results.

2. Building extraction

The building extraction task involves separating buildings from ground, trees, and other objects (e.g. cars, lamps etc.). This paper extract building points by removing non-building points step by step. Firstly, apparent tree and wall points are removed. Secondly the region growing algorithm is employed to detect ground points. Finally, the connective component analysis is used to separate buildings from remaining trees.

2.1. Removing apparent trees and walls

In terms of the building detection task, non-building points, including trees and walls, are viewed as noises. These points usually locate near the building points and thus affect the computation of their features as feature calculation of points is usually performed within their neighborhood. Therefore, these points should be firstly removed before computing features which are used in drectly detecting building points. The normal vector and the multi-return feature are utilized to remove these apparent noises.

The normal of a point on the surface is estimated as the normal of a plane tangent to the surface. Therefore, the normal of a point can be derived by performing PCA (Principal Component Analysis) on the covariance matrix determined by the neighbors of this point. For each point, the covariance matrix C is defined as:

$$C = \frac{1}{k}\sum_{i=1}^{k}\left(p_i - \overline{p}\right)\left(p_i - \overline{p}\right)^T \tag{1}$$

where k denotes the number of neighbors of the point, p_i refers to the i-th neighbor and $\overline{p}$ is the centroid of all the neighbors. The normal of a point is defined as the eigenvector corresponding to the minimum eigenvalue. If the point and its neighbors are on a plane, its normal is parallel to the normal of the plane.

In the real world, normals of building roofs are impossible to be perpendicular to the z-axis with the orientation e_z (0,0,1) while normals of wall points are usually orthogonal to the z-axis. Therefore, apparent wall points can be detected by comparing their normals with e_z.

After removing wall points, apparent tree points are identified by the multi-return feature. As the laser beam is able to penetrate trees, tree points contain many multi-return points. Meanwhile, buildings and grounds usually have only one return. Therefore, it can be concluded that points demonstrating high multi-return features are very likely to be tree points rather than building points. There are various ways of computing multi-return features and they have a high correlation with each other. In this paper, the multi-return feature f_{mr} is estimated as:

$$f_{mr} = \frac{\sum_N \left(p_i > 1\right)}{\sum_N p_i} \tag{2}$$

where p_i denotes a point with the i-th return number, N is the neighborhood of a point. The numerator counts the number of points whose return number is larger than 1 while the denominator refers to the total number of points. For most building and ground points, f_{mr} is nearly zero as fewer

multi-return points exist. On the contrary, tree points usually have high values of f_{mr} as there are many points whose return number is superior to 1 because of the penetration of the laser beam. In short, the multi-feature f_{mr} is able to detect apparent tree points.

2.2. Removing ground points

After removing apparent noises, the region growing algorithm based on geometric features is utilized to identify ground points. In the point clouds collected by airborne LiDAR system, ground surface is usually smooth and huge with the largest connected area. Thus the region growing algorithm aims to detect smooth surface is employed to separate ground points. Since points on the same smooth surface usually have similar normals, the region growing algorithm employs the normal to find smooth surfaces.

This region growing algorithm can also detect isolated outliers. Due to flying objects (e.g., birds and aircrafts) and LiDAR system errors, there are high and low outliers in the point clouds. For the isolated high or low outliers, they are usually grouped into clusters with fewer points. Thus by eliminating clusters with a small number of points, these outliers are removed. In addition, some tree points which do not form smooth surfaces are also identified as outliers.

2.3. Building points detection

After removing apparent walls and trees and ground, the remaining points mainly contain buildings and trees. As buildings and trees are usually located separately, the connected component analysis is carried out to classify these points into separate groups in Euclidean space. Then geometric features, i.e. the area, the ratio of width to height, the average point density, are calculated to removing trees. At last building points are identified by the ratio of points whose curvatures are of high values.

The curvature of a point is estimated as a relationship between the eigenvalues of the covariance matrix C, as:

$$\sigma = \lambda_0 / \left(\lambda_0 + \lambda_1 + \lambda_2 \right) \tag{3}$$

where $\lambda_0, \lambda_1, \lambda_2 \left(\lambda_0 < \lambda_1 < \lambda_2 \right)$ denote the eigenvalues of the covariance matrix C. If the point and its neighboring points belong to a planar roof, σ is nearly zero as the minimum eigenvalue is nearly zero. Otherwise, if a point lies on a tree, σ is larger than zero. Since building points contain a sufficient number of points with lower values of σ, by comparing the ratio of points with higher values of σ, building points can be separated from tree points .

3. Roof segmentation

In order to separate building roofs, the region growing algorithm utilizing the normal and curvature is performed for each building. Since the planar clusters are preferred rather than smooth surfaces, smaller normal threshold is used and seed points with lower curvature are preferred.

In order to correctly separate roof neighbourings, non-planar points whose curvatures are larger than a threshold are firstly identified and removed before the following region growing clustering. The roof neighboring points and outliers (shown in figure 1(b)) belong to non-planar points as their neighborhoods contains either points from several planar roofs or fewer points. On the contrary, points around the center of roofs are planar points because their neighboring points belong to the same plane and thus their curvatures are very small. Apart from owning higher curvatures, non-planar points also have different values of normal compared with their corresponding plane as their neighborhood includes points from other planar roofs. Therefore, in order to correctly classify these points, non-planar points shoubl be removed before performing the region growing algorithm.

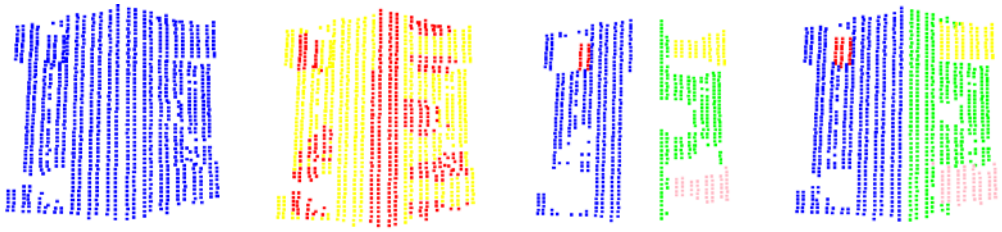

(a) (b) (c) (d)

Figure 1. Roof segmentation

After the non-planar points are removed, the region growing algorithm is carried out to find planar clusters. Smaller normal threshold is imposed to make sure that planar clusters of high quality are obtained. As points with higher curvatures are already removed, the remaining points have lower curvatures and correct normal and thus can be correctly classified by the region growing algorithm as shown in figure 1(c).

After the region growing algorithm, non-planar points with higher curvatures are then assigned to the corresponding planar clusters. The distance of the point to the plane and the minimal distance between the point and points of the plane are both taken into consideration to ensure that the point is assigned to the correct plane. At last, building roofs are correctly separated as displayed in figure 1(d).

4. Model generation

3D building models acquired from airborne LiDAR data are composed of minimum segments which include building outlines and roof intersections. Thus the model generation process involves obtaining regular building outlines from building points and estimating the roof intersection segments based on the roof segmentation results. By combining those elements, 3D building models are derived.

Due to the shortage of laser scanner in capturing linear features, obtained building boundary points usually display as zigzag [13]. In order to obtain geometrically correct building models, the boundary regularization, including boundary points detection, segments extraction and segments adjustment, is performed. Firstly, the building boundary points are extracted by the 2D alpha shape algorithm which is able to correctly extract boundary points of both convex and concave shapes of buildings. Secondly, the RANSAC algorithm [14] combined with the connected component analysis is performed to extract long segments. At last by adopting the adjustment suggested in [12] to adjust those segments, regular and geometrically correct building outlines are obtained.

Meanwhile, the roof intersections are estimated by intersecting the separated planar roofs. By combining the regularized outlines and roof intersection segments, key vertices and intersection segments are determined and the final 3D building models are acquired.

5. Experiments and results

In this paper, the Vaihingen dataset provided by the German Association of Photogrammetry and Remote Sensing (DGPF) [15] is employed to provide both quantitative and qualitative evaluation of our method. The DGPF data set is acquired on 21 August 2008 by Leica Geosystems using a Leica ALS50 system with 45° field of view and a mean flying height above ground of 500m. The mean point density is 4 points/m^2. The dataset of Area 2 which is a characterized by a few high-rising residential buildings that are surrounded by trees is utilized in this paper.

Figure 2 shows the classification results of building extraction. As shown in figure 2(b), wall points (in yellow) are correctly detected. Even though some non-wall points (e.g. tree points) are also extracted, this false classification does not affect the extraction of buildings and thus can be neglected. After wall points are removed, as shown in figure 2(c), apparent tree points (in green) are extracted according to the multi-return feature. Then the region growing algorithm is carried out to extract smooth surfaces and the cluster with the largest area is classified as ground (brown points in figure 2(c)). Meanwhile, clusters with fewer points are labelled as noises which are red points in figure 2(c).

At last, building points (figure 2(d)) are extracted by utilizing the connected component analysis as well as the ratio of points with high values of curvature.

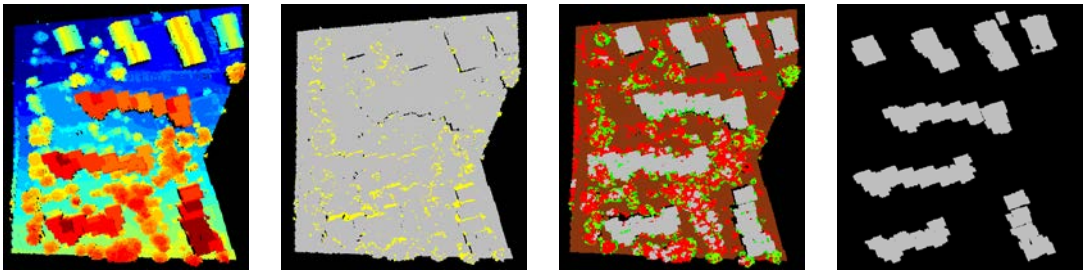

(a) (b) (c) (d)

Figure 2. Flow chart of building extraction.

To evaluate the accuracy of the roof segmentation results (figure 3(a)) and the final building models (figure 3(b)), the mean and standard deviation of the distance of the points to their corresponding planes are computed. The mean value is 0.022 m while the standard deviation is 0.001 m, which indicates that points belonging to a cluster are nearly within a plane. Lower values of mean and standard deviation also prove that the roof segmentation method is able to obtain planar clusters with high quality and accuracy. Since building models are reconstructed based on these segmentation results, it can be concluded that the final building models also display high accuracy of in terms of the distance of points to the models.

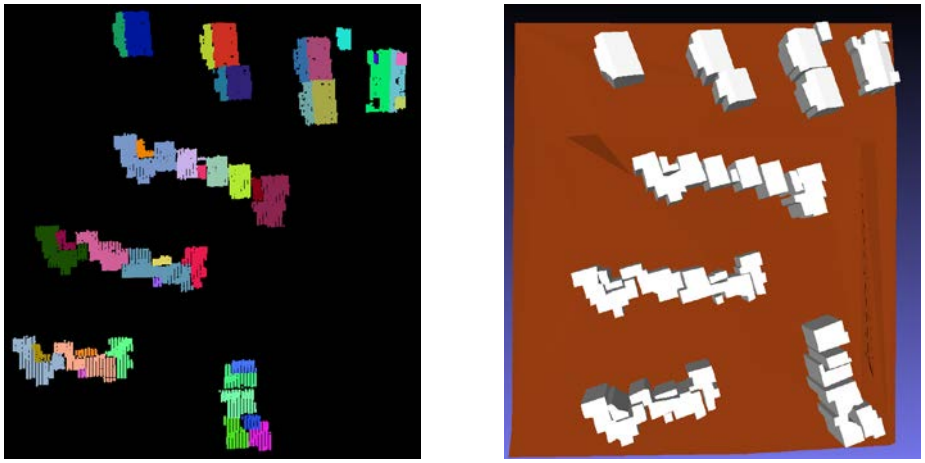

(a) Roof segmentation resutls, each planar roof is rendered in a random color.

(b) Final 3D building models, the building models are rendered in white while the ground surface brwon.

Figure 3. Roof Segmentation results and building modelling results.

6. Conclusions and future work

This paper presents a framework of obtaining 3D building model from airborne LiDAR data. This framework is totally automatic while having less reliance on parameter tuning. In addition, experimental results demonstrate that the building detection method is able to effectively remove non-building points and thus detect building points correctly. Moreover, the roof segmentation results obtain high quality and accuracy of planar clusters, which ensures the accuracy of the final building models. In future work, we will apply this framework to other dataset in order to improve its applicability.

Acknowledgments
This research is supported by "Hundred Talents Program" of the Chinese Academy of Sciences and Project 41171265 supported by National Natural Science Foundation of China. The Vaihingen data set was provided by the German Society for Photogrammetry, Remote Sensing and Geoinformation (DGPF) [15]: http://www.ifp.uni-stuttgart.de/dgpf/DKEP-Allg.html (in German).

References
[1] Maas H G and Vosselman, G 1999 *ISPRS J. of Photogramm. and Remote Sens.* **2** 153-163
[2] Alharthy A and Bethel J 2002 *Int. Archives of Photogramm. Remote Sens. and Spatial Infor. Sciences* **34** 29-34
[3] Mallet C, Bretar F, and Soergel U 2008 *Photogrammetrie Fernerkundung Geoinfor.* **5** 337-349
[4] Meng X, Wang L, and Currit N 2009 *Photogramm. Eng. and Remote Sens.***75** 437-42
[5] Yun Y and Ying L 2009 *Urban Remote Sens. Event Joint* 1-6
[6] Rabbani T and Van Den Heuvel F 2005 *ISPRS WG III/3, III/4*, 2005, **3**, pp. 60-65
[7] Schnabel R, Wahl R, and Klein R 2007 *Computer Graphics Forum* **26** 214-26
[8] Tarsha-Kurdi F, Landes T, and Grussenmeyer P 2008 *Photogramm. J. of Finland* **21** 97-109
[9] Sampath A and Shan J 2010 *IEEE Trans. on Geoscience and Remote Sens.***48** 1554-67
[10] Sampath A and Shan J 2007 *Photogramm. Eng. and Remote Sens.* **73** 805 -812
[11] Wei S, Jin Z, and Feng Y 2011 *19th Int. Conf. on Geoinformatics* 1-4
[12] Zhang K, Yan J and Chen S C 2006 *IEEE Trans. on Geoscience and Remote Sens.* **44** 2523-33
[13] Zhou Q Y and Neumann U 2008 *Proc. of the 16th ACM SIGSPATIAL Int. conf. on Advances in GIS* 43-50
[14] Fischler M A and Bolles R C 1981 *Commun. of the ACM* **24** 381-395
[15] Cramer M 2010 *Photogrammetrie – Fernerkundung – Geoinformation* **2** 73-82